

Electronic supplementary information

**Selective hydrogenation of CO<sub>2</sub> to CH<sub>4</sub> over two-dimensional nickel silicate  
molecular sieves†**

Hyung-Ki Min,<sup>a,‡</sup> Haehyun Min,<sup>b,‡</sup> Sungjoon Kweon,<sup>c</sup> Young Woo Kim,<sup>d</sup> Siyeon Lee,<sup>c</sup> Chae-Ho  
Shin,<sup>\*d</sup> Min Bum Park<sup>\*c</sup> and Sung Bong Kang<sup>\*b</sup>

<sup>a</sup>*LOTTE Chemical Research Institute, Daejeon 34110, Korea*

<sup>b</sup>*School of Earth Sciences and Environmental Engineering, Gwangju Institute of Science and  
Technology, Gwangju 61005, Korea*

<sup>c</sup>*Department of Energy and Chemical Engineering, Incheon National University, Incheon 22012,  
Korea*

<sup>d</sup>*Department of Chemical Engineering, Chungbuk National University, Cheongju, Chungbuk  
28644, Korea*

†Electronic supplementary information (ESI) available. See DOI: xxx

‡These authors contributed equally to this work.

\*Corresponding authors: chshin@chungbuk.ac.kr (C.-H.S.); mbpark@inu.ac.kr (M.B.P.);  
sbkang@gist.ac.kr (S.B.K.)

**Table S1** Binding energies of XPS spectra for the catalysts employed in this study

| Catalyst   | Binding energy (eV)               |                                   |       | $\Delta E_{\text{Ni-Si}}^b$ |
|------------|-----------------------------------|-----------------------------------|-------|-----------------------------|
|            | Ni 2p <sub>1/2</sub> <sup>a</sup> | Ni 2p <sub>3/2</sub> <sup>a</sup> | Si 2p |                             |
| Ni-DML-100 | 873.8                             | 856.2                             | 103.2 | 753.0                       |
| Ni-DML-120 | 874.1                             | 856.2                             | 103.1 | 753.1                       |
| Ni-DML-140 | 874.1                             | 856.6                             | 103.6 | 753.0                       |
| Ni-DML-160 | 874.3                             | 856.6                             | 102.6 | 754.0                       |
| Ni-DML-180 | 873.9                             | 856.4                             | 102.9 | 753.5                       |
| Ni/B-MWW   | 876.0 (32)                        | 856.5 (36)                        | 103.5 | 753.0                       |
|            | 872.9 (68)                        | 854.5 (64)                        |       | 751.0                       |

<sup>a</sup> The values in parentheses indicate the relative area ratios. <sup>b</sup> Difference in Ni 2p<sub>3/2</sub> and Si 2p binding energies.

**Table S2** Comparison of TOF for catalysts prepared in this and previous studies

| Catalyst   | CO <sub>2</sub> hydrogenation conditions |  |   | Ref.       |
|--|--|--|---|------------|
|  | Temp. (°C)                               | GHSV (cm <sup>3</sup> g <sub>-cat.</sub> <sup>-1</sup> h <sup>-1</sup> ) | TOF (CO <sub>2</sub> ) (s <sup>-1</sup> ) |            |
| Ni-DML-100   | 330                                      | 84,000   | 0.008                                     | This study |
| Ni-DML-120   | 330                                      | 84,000   | 0.010                                     | This study |
| Ni-DML-140   | 330                                      | 84,000   | 0.079                                     | This study |
| Ni-DML-160   | 330                                      | 84,000   | 0.025                                     | This study |
| Ni-DML-180   | 330                                      | 84,000   | 0.012                                     | This study |
| 5 wt.% Ni/B-MWW  | 330                                      | 84,000   | 0.051                                     | This study |
| 5 wt.% Ni/Al <sub>2</sub> O <sub>3</sub>                     | 330                                      | 84,000   | 0.046                                     | This study |
| 12 wt.% Ni/Al <sub>2</sub> O <sub>3</sub>                    | 275                                      | 10,000   | 0.060                                     | 40         |
| 5 wt.% Ni/SiO <sub>2</sub>                                   | 300                                      | 6,000  | 0.103                                     | 41         |
| 5 wt.% NiRu/SiO <sub>2</sub>                                 | 300                                      | 6,000  | 0.087                                     | 41         |
| 10 wt.% NiRu/SiO <sub>2</sub>                                | 300                                      | 6,000  | 0.044                                     | 41         |
| 5 wt.% Ni/SiO <sub>2</sub>                                   | 350                                      | 22,000   | 0.076                                     | 42         |
| 5 wt.% Ni/Al <sub>2</sub> O <sub>3</sub>                     | 300                                      | 6,000  | 0.063                                     | 43         |
| 5 wt.% Ni <sub>3</sub> Fe/Al <sub>2</sub> O <sub>3</sub>     | 300                                      | 6,000  | 0.083                                     | 43         |
| 3.4 wt.% NiRh <sub>0.1</sub> /Al <sub>2</sub> O <sub>3</sub> | 300                                      | 6,000  | 0.037                                     | 43         |
| NiMgAl   | 350                                      | 2,400  | 0.034                                     | 44         |
| Ru/NiMgAl  | 350                                      | 2,400  | 0.034                                     | 44         |

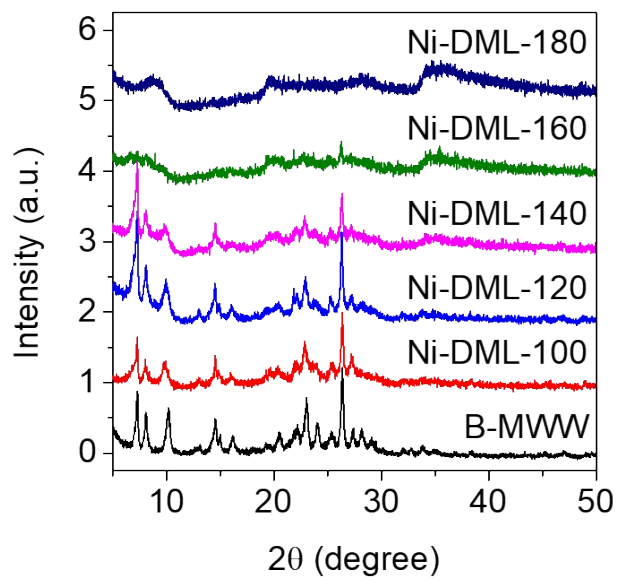


**Fig. S1** Powder XRD patterns of calcined B-MWW and Ni-DML- $x$  ( $x = 100\text{--}180$  °C) catalysts.

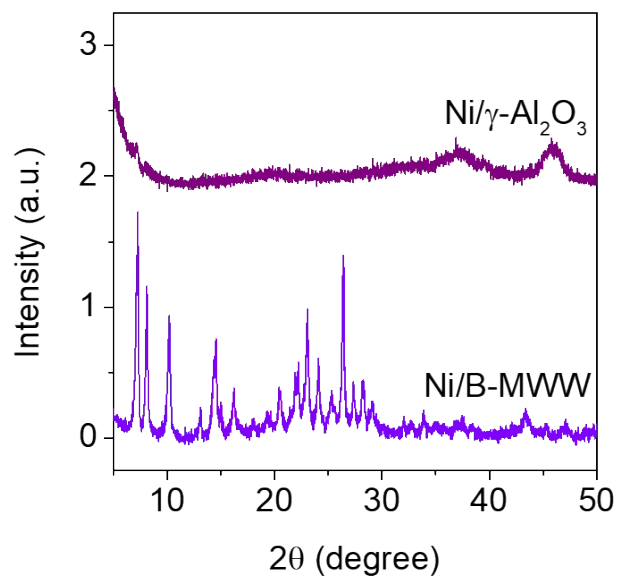


**Fig. S2** Powder XRD patterns of calcined  $\text{Ni}/\text{B-MWW}$  and  $\text{Ni}/\gamma\text{-Al}_2\text{O}_3$  catalysts.

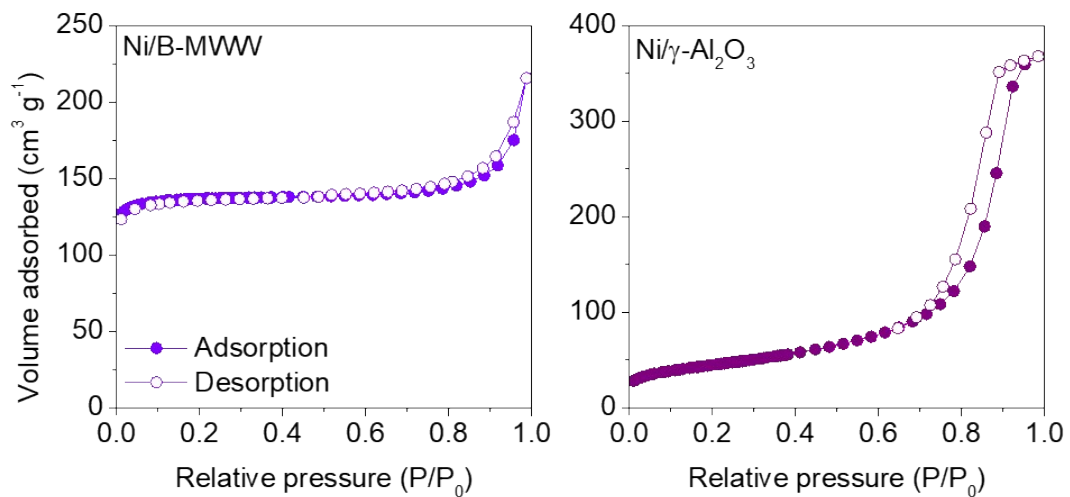


**Fig. S3** N<sub>2</sub> sorption isotherms of Ni/B-MWW and Ni/γ-Al<sub>2</sub>O<sub>3</sub> catalysts.

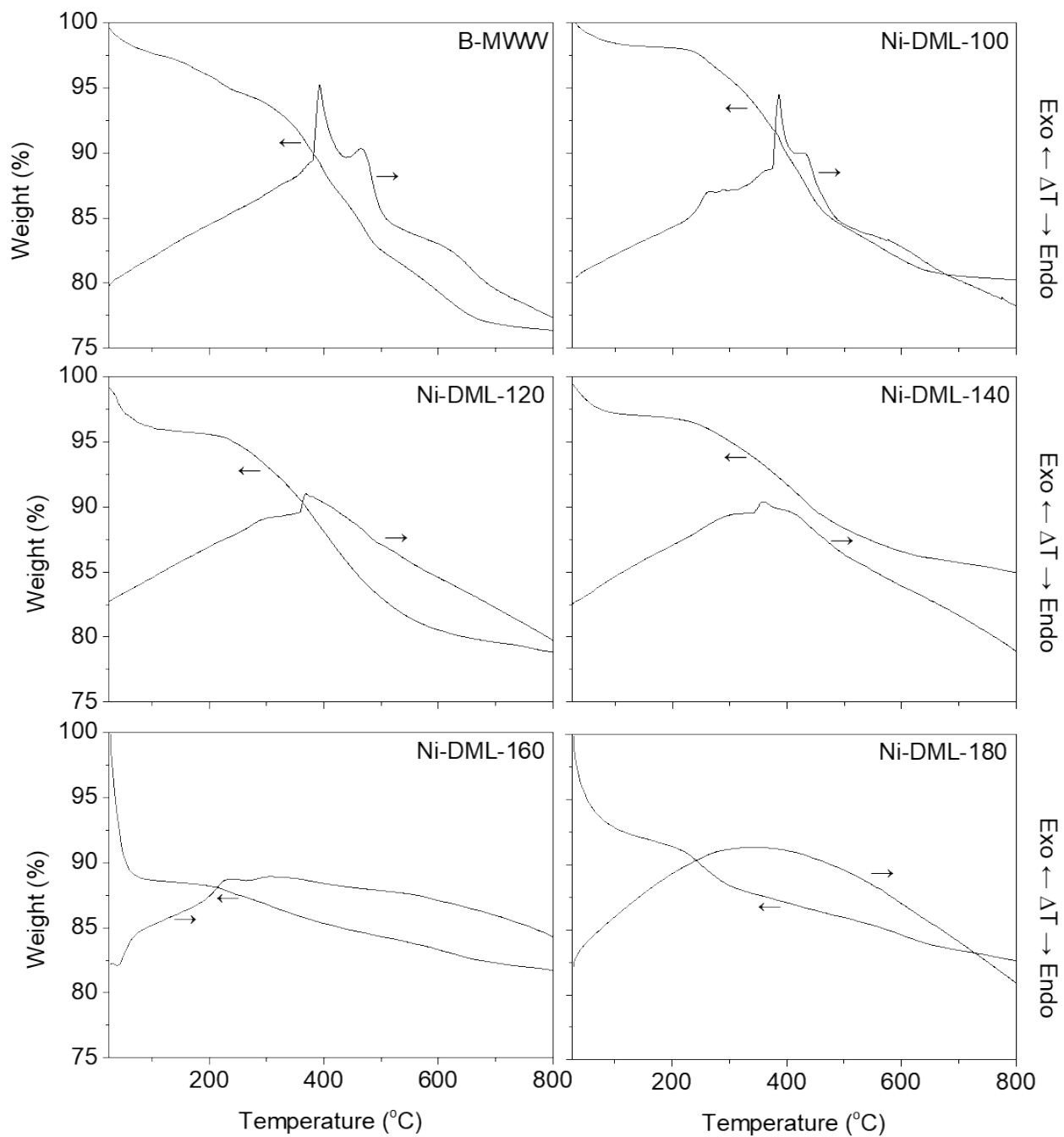


**Fig. S4** TGA/DTA curves of as-synthesized B-MWW and Ni-DML- $x$  ( $x = 100-180$  °C) samples.

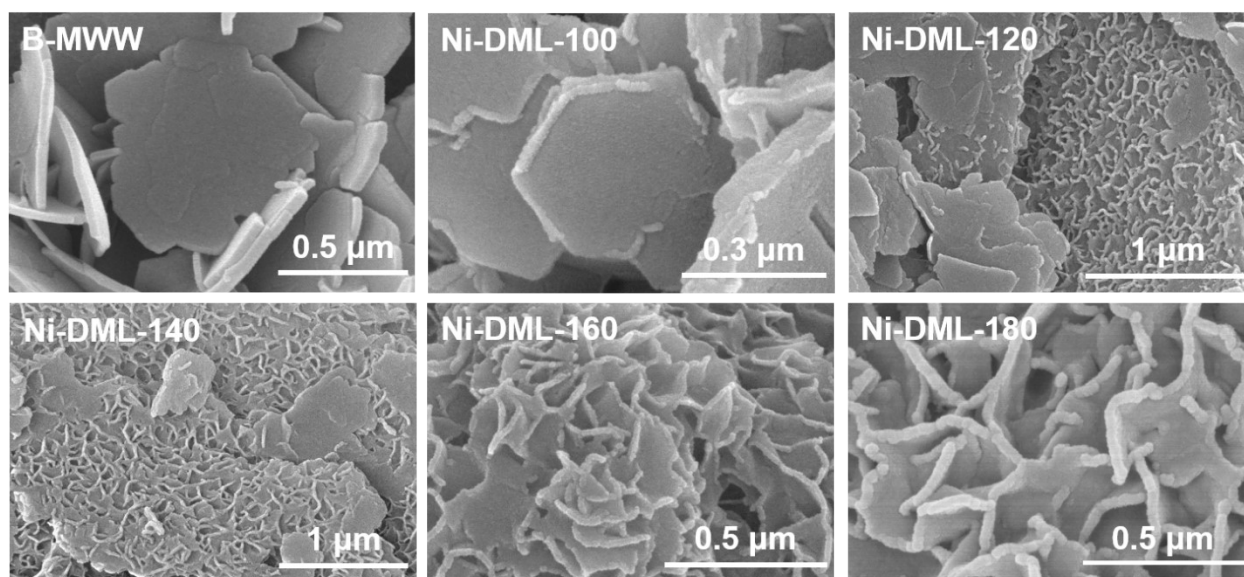


**Fig. S5** SEM images of B-MWW and Ni-DML- $x$  ( $x = 100\text{--}180$  °C) catalysts.



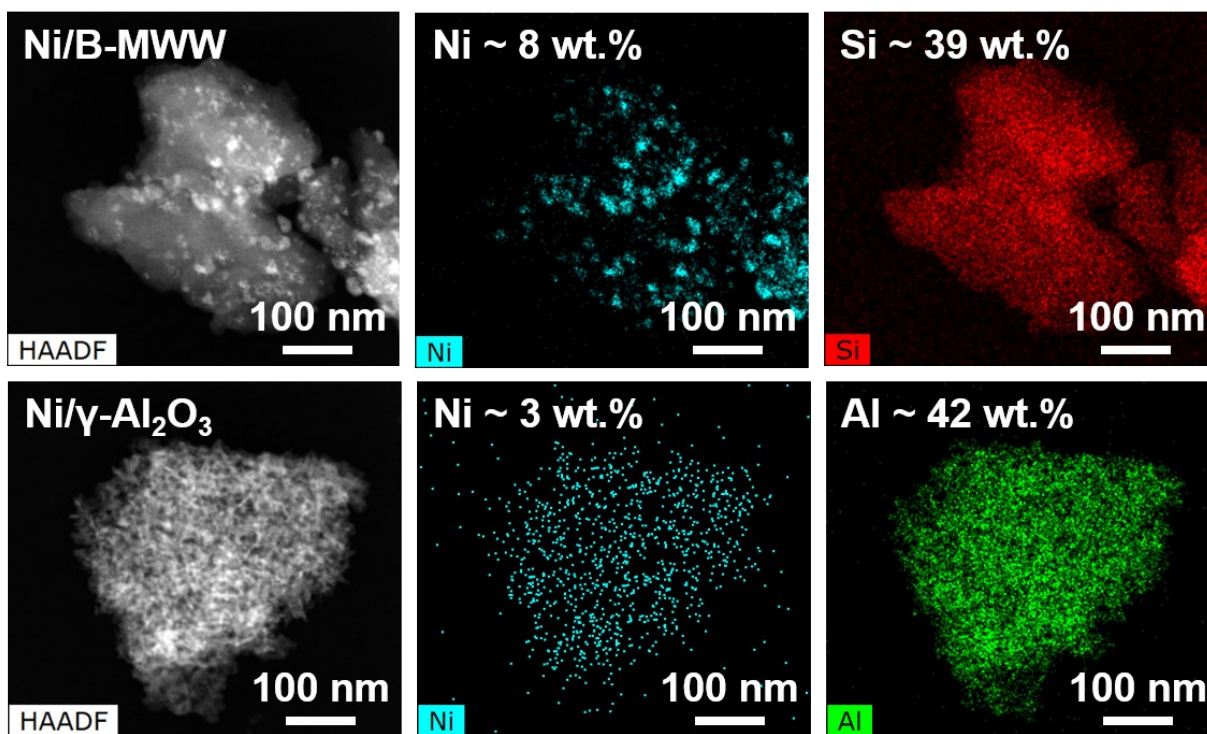


**Fig. S6** STEM-EDS images of Ni/B-MWW and Ni/γ-Al<sub>2</sub>O<sub>3</sub> catalysts.

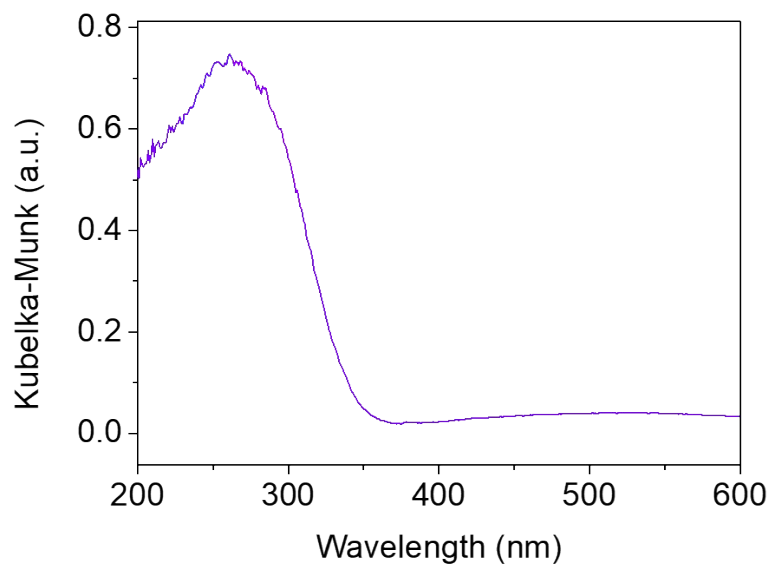


**Fig. S7** UV-DRS spectrum of Ni/B-MWW catalyst.

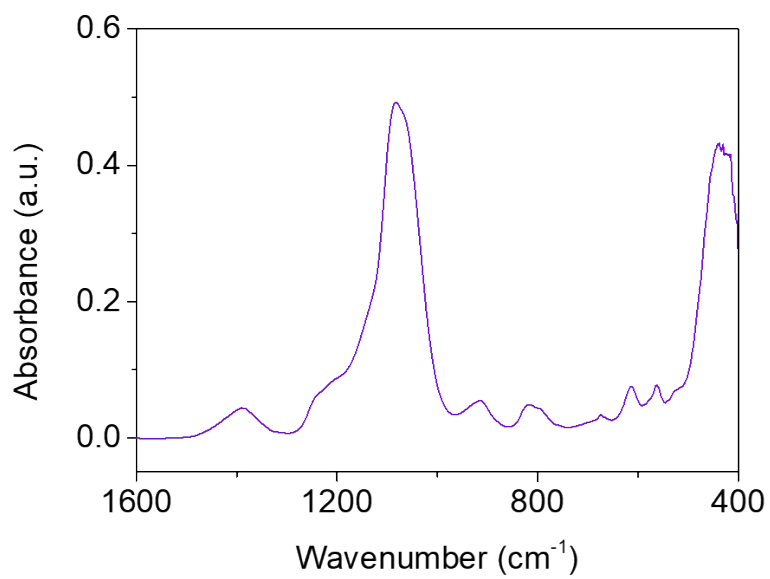


**Fig. S8** IR spectrum in the structural region of the Ni/B-MWW catalyst.

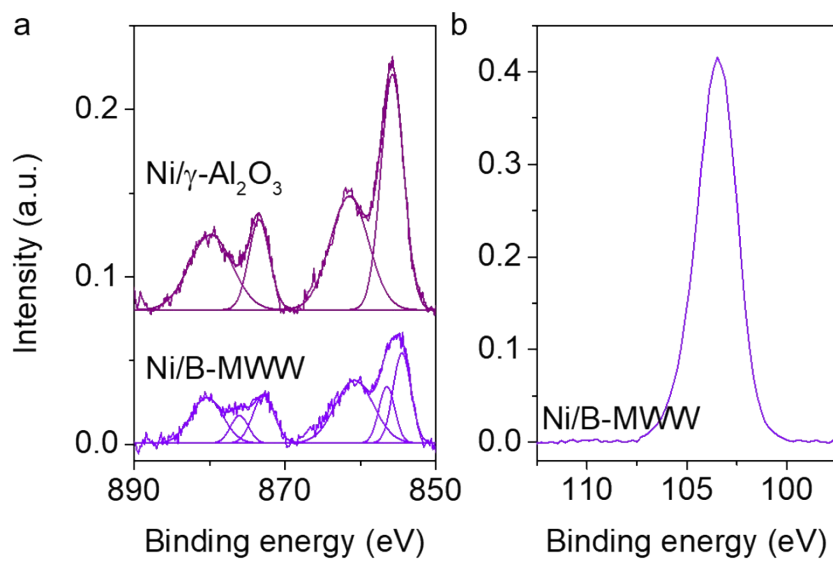


**Fig. S9** (a) Ni 2p XPS and (b) Si 2p XPS spectra for Ni/B-MWW and/or Ni/ $\gamma$ -Al<sub>2</sub>O<sub>3</sub> catalysts.

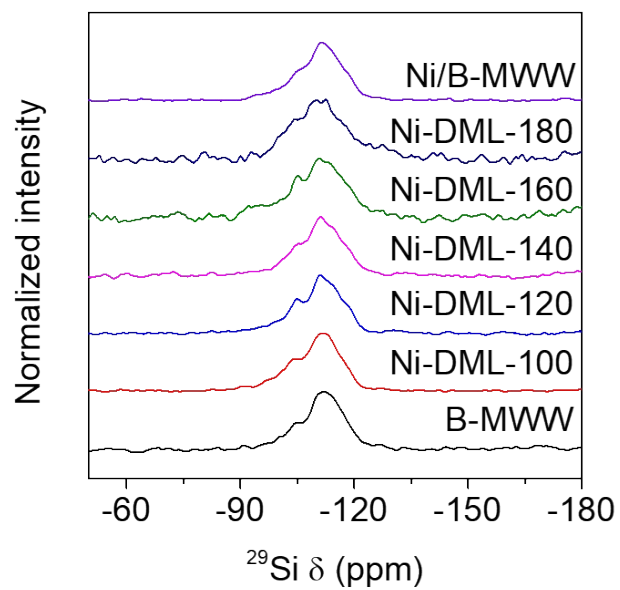


**Fig. S10**  $^{29}\text{Si}$  MAS NMR spectra of B-MWW, Ni-DML- $x$  ( $x = 100\text{--}180$  °C), and Ni/B-MWW catalysts.

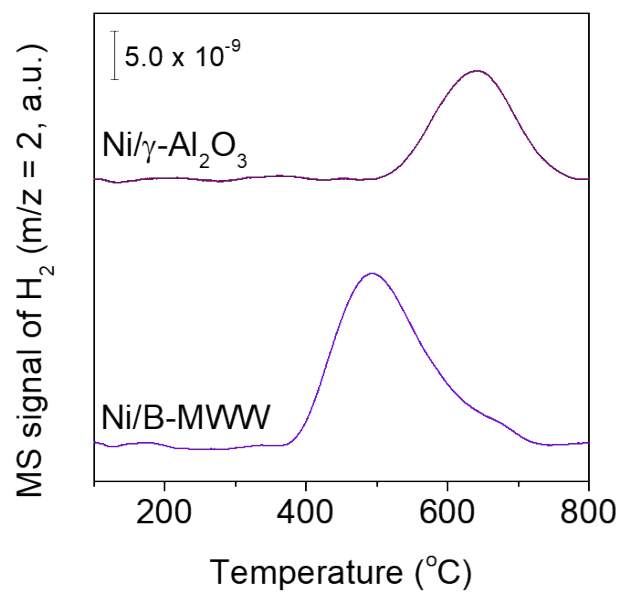


**Fig. S11** H<sub>2</sub> TPR profiles of Ni/B-MWW and Ni/γ-Al<sub>2</sub>O<sub>3</sub> catalysts.

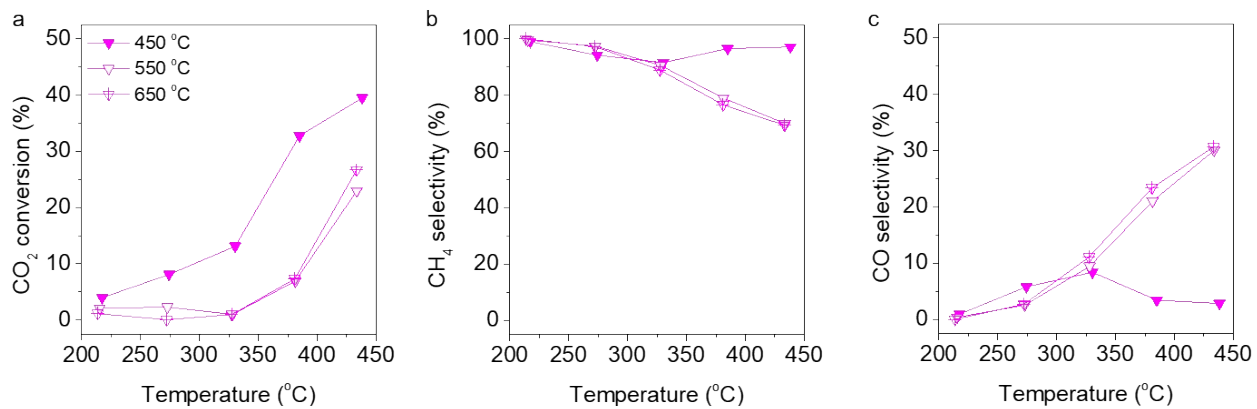


**Fig. S12** (a) CO<sub>2</sub> conversion, (b) CH<sub>4</sub> selectivity, and (c) CO selectivity of Ni-DML-160 catalyst pre-reduced with 80 vol.% H<sub>2</sub> (Ar balance) at different temperatures (450–650 °C) as a function of reaction temperature at a GHSV of 30,000 h<sup>-1</sup> for 1.5 h at each temperature.

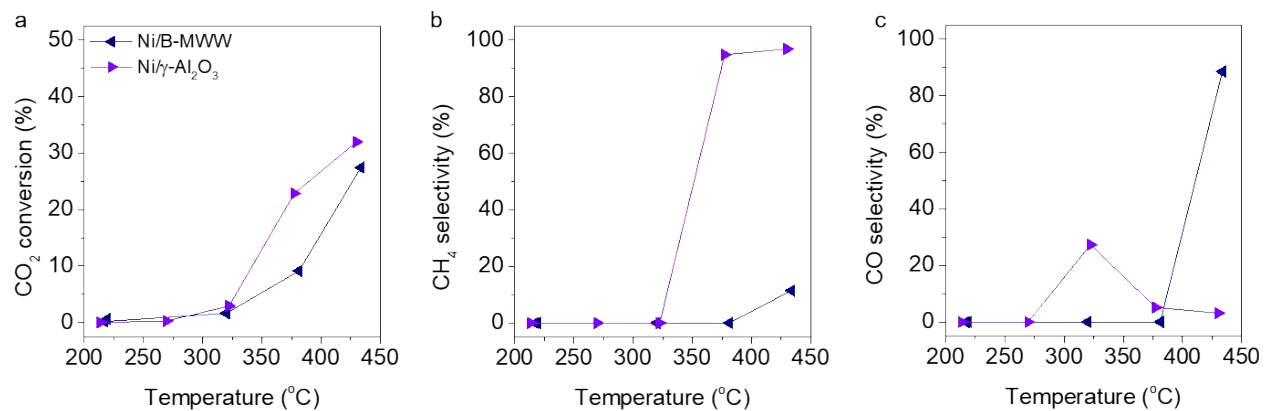


**Fig. S13** (a) CO<sub>2</sub> conversion, (b) CH<sub>4</sub> selectivity, and (c) CO selectivity of Ni/B-MWW and Ni/ $\gamma$ -Al<sub>2</sub>O<sub>3</sub> catalysts as a function of reaction temperature at a GHSV of 30,000 h<sup>-1</sup> for 1.5 h at each temperature. The catalysts were routinely pre-reduced with 20 vol.% H<sub>2</sub> (Ar balance) at 450 °C for 1 h.



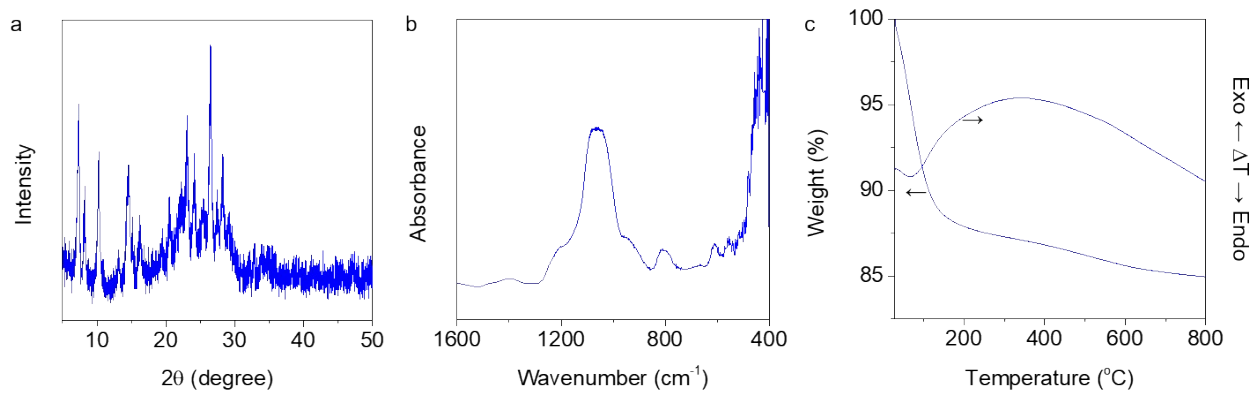


**Fig. S14** (a) Powder XRD pattern, (b) IR spectrum in the structural region, and (c) TGA/DTA curves of the Ni-DML-140 catalyst after reaction.